Chemistry & Biology
Brief Communication

Inverse In Silico Screening for Identification of Kinase Inhibitor Targets

Stefan Zahler,[1,5] Simon Tietze,[2] Frank Totzke,[3] Michael Kubbutat,[3] Laurent Meijer,[4] Angelika M. Vollmar,[1] and Joannis Apostolakis[2,5,*]
[1]Pharmaceutical Biology, Department of Pharmacy, University of Munich, Germany
[2]Bioinformatics Group, Department of Computer Science, University of Munich, Germany
[3]ProQinase GmbH, Tumor Biology Center Freiburg, Germany
[4]CNRS Station Biologique de Roscoff, France
[5]These authors contributed equally to this work.
*Correspondence: joannis.apostolakis@ifi.lmu.de
DOI 10.1016/j.chembiol.2007.10.010

SUMMARY

Protein kinases are clinically relevant, attractive drug targets for cancer. One major problem with kinase inhibitors is broad promiscuity, causing off-target actions and side effects. In silico prediction of targets of a compound would immensely facilitate and accelerate drug development. Using a virtual "inverse" screening approach, where single compounds are docked into protein structures from a database, we identify among known targets of indirubin derivatives phosphoinositide-dependent kinase 1 (PDK1) as a target of one derivative (6BIO) in particular. This prediction is functionally supported by an in vitro kinase assay, inhibition of intracellular phosphorylation of PDK1-substrates, and inhibition of endothelial cell migration, which highly depends on PDK1. Virtual inverse screening combined with biological tests, thus, is proposed as a valuable tool for the drug discovery process and re-examination of already established kinase inhibitors.

INTRODUCTION

During the last years, protein kinases have been recognized as central drug targets for tumor therapy [1]; among the successfully targeted ones are MAP kinases [2], receptor tyrosin kinases [3], and kinases of the PI3-kinase/Akt/mTOR signaling pathway [4, 5]. This progress was considerably boosted by the clinical success of small molecular inhibitors, like Gleevec (Novartis) or Iressa (AstraZeneca). One problematic issue with kinase inhibitors is specificity since they generally bind at the relatively conserved ATP binding pocket of the kinase family [6, 7]. However, it has also recently been suggested that the biological activity of kinase inhibitors may rely on a multispecific inhibition of different kinases [8]. In order to be able to judge both positive and negative effects of multispecificity, it is necessary to reliably identify the cellular targets of inhibitors. Conventionally, kinase inhibitor activity and specificity is tested in vitro within a defined panel of isolated kinases [6]. This approach, however, has the limitation that potential targets of the compound tested may be overlooked, if they are not in the panel. In addition, medium or high throughput testing of different compounds against a comprehensive panel of kinases is resource intensive, and the results still need to be confirmed in cellular assays and in vivo. Conventional structure based in silico approaches do not address specificity, as in general, only one target is tested against different compounds of interest. Thus, some other, more-relevant target structure may be overlooked. "Inverse screening," where a single compound is docked into different protein structures that are documented in protein databases, has been suggested [9, 10] and was recently applied by us to the problem of artificial receptor design [11]. Such an approach has the advantage that it can in principle be applied on large numbers of compounds and, thus, be used already at the discovery stage of drug-development projects. However, to our knowledge, inverse screening has to date neither been proven in practice nor has it been tested for its accuracy within a large family of proteins. We here use inverse screening to identify kinase targets for three derivatives of indirubin (Figure 1G), namely 5-bromo-indirubin-3′oxime (5BIO), 6-bromo-indirubin-3′oxime (6BIO), and 7-bromo-indirubin-3′oxime (7BIO). All three compounds are derivatives of indirubin, a trace isomer of the indigo dye. Indirubin has been identified as active principle in a traditional Chinese medicine against chronic myelogenous leukemia (CML) with various biological effects on a cellular basis [12]. Due to its poor solubility in water, indirubin is no longer in clinical use [13], but a vast number of derivatives have been generated as anticancer drugs and scaffolds for kinase inhibitors [14, 15]. Although the three compounds are structurally very similar, their biological effects differ largely [16]: while 5BIO and 6BIO seem to be inhibitors of CDKs, of GSK-3β, and other kinases, 7BIO causes cell death without affecting any kinase that has so far been investigated in this context [16]. Employing these compounds, we are able to test the principle of inverse screening, and to assess whether it allows the identification of ligand specific effects at the same time.

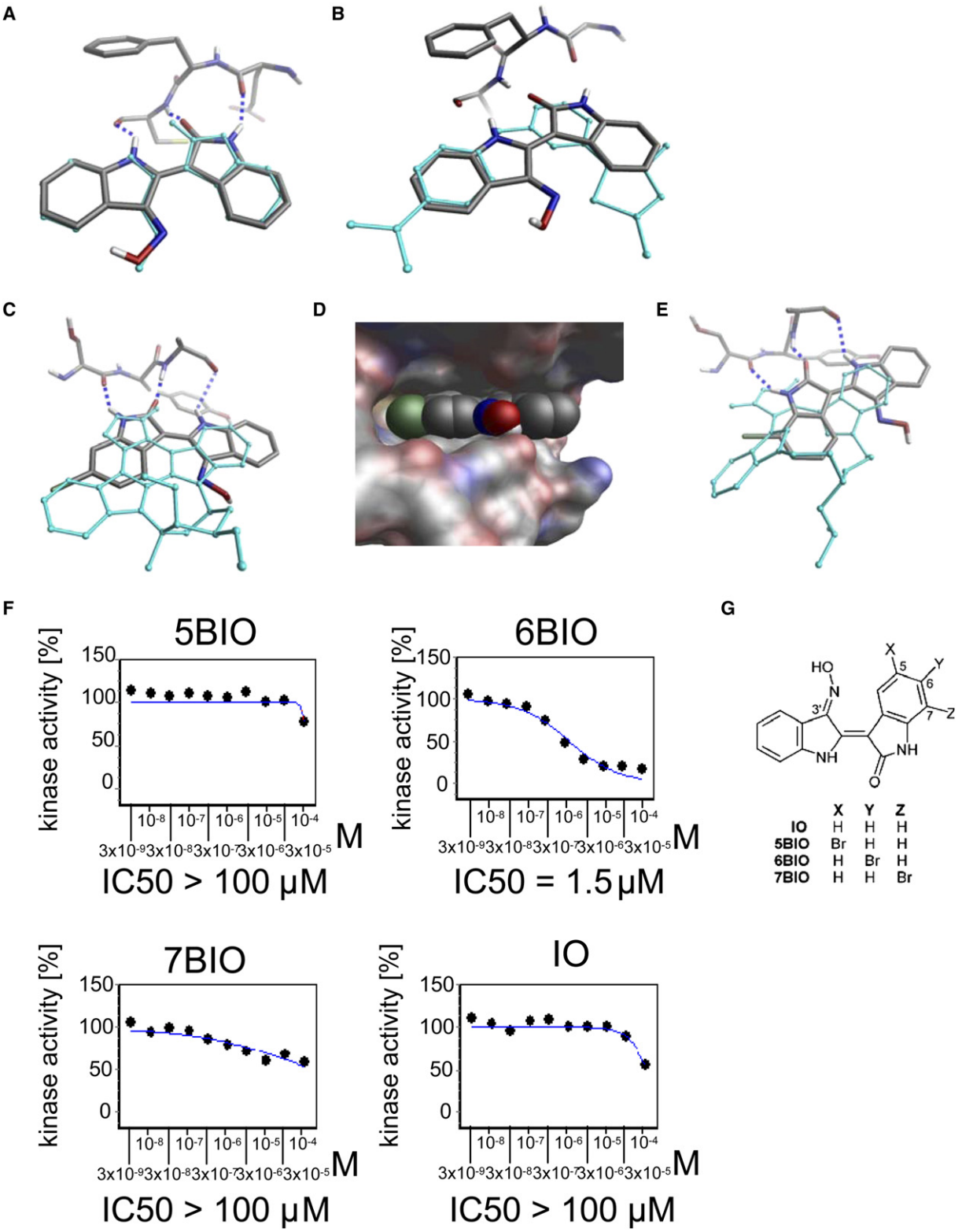

Figure 1. Docking Results and In Vitro Kinase Assay

(A) Indirubin 3′-oxime (thick, atom colored sticks) redocked into a CDK5 structure in complex with indirubin 3′-oxime. The resulting score leads to rank 11 for this structure among the kinases and 36 in the complete set of complexes. The model is in perfect agreement with the typical interaction motif of two or three hydrogen bonds (shown as dashed blue lines) to the protein backbone (shown in the background of this picture). The conformation of indirubin 3′-oxime as found in the PDB structure is shown as thin cyan sticks and shows nearly perfect agreement with the model.

RESULTS AND DISCUSSION

Indirubin-3′-oxime (IOX) and the three derivatives were screened against our database of ~6,000 protein binding sites. Visual examination of single docking results confirmed the known docking poses and essential interactions for these compounds in kinases (Figures 1A and 1B).

The results of the virtual inverse screening for the three indirubin derivatives with all protein binding sites are shown in Table S1 (see the Supplemental Data available with this article online). The extracted data for kinase structures are summarized in Table 1. Virtual inverse screening for 5BIO, 6BIO and IOX shows significant enrichment of their well known targets (CDK2, CDK5, GSK-3β) in the top 1%: overall there are 62 structures of these proteins in the database. The corresponding enrichment factors at 1% lie between 16 (5BIO, IOX) and 20 (6BIO). For 6BIO and IOX, at least one representative for each of its known targets is found among the 20 best ranked structures. CDK5 in 5BIO is a false negative as it does not appear among the 300 best ranked structures.

We identified kinases that ranked well for all three halogeno-indirubins: CSK2A, WEE1, CDC2H, RIFK, KSYK, and PDK1 (Table 1). Since WEE1 is a cell-cycle-associated kinase [17], functional differentiation from effects on CDK2 or CDK5 is hardly possible. RIFK is riboflavin kinase, which has no known signal transduction activity. From the remaining four, we selected PDK1 for experimental validation. PDK1 shows the most significant differences in the rankings especially between 5BIO and 6BIO, and is a therapeutically extremely interesting target [18, 19] for which inhibitors are still rare. PDK1 is downstream of the PI3 kinase and controls many central signaling pathways by phosphorylating the Akt kinase and the p70S6 kinase, thereby regulating cell growth and survival [20]. Consequently, PDK1 knockout animals are not viable [20], and increased PDK1 activity is associated with tumor cells [19]. Recently, a further important role for PDK1 has been identified: the control of motility both in tumor cells [18, 21] and in endothelial cells [22–24]. Thus, inhibitors of PDK1 might attack tumors directly (reduction of tumor cell survival and proliferation), reduce metastasis (by depressing motility of tumor cells), and inhibit tumor angiogenesis. Finally, PDK1 plays an important role in regulating T cell development [25], highlighting both the risks of targeting PDK1 for cancer therapies and the possibility of addressing T cell related diseases through inhibitors of PDK1.

Figure 1C depicts the modeled complex of 6BIO in PDK1, which displays perfect interaction geometries. The binding pocket of PDK1 can easily accommodate the additional bromine atom (Figure 1D). In contrast, only poor interaction geometries are found between 7BIO and PDK1 (Figure 1E), which led to a low ranking (#184). 5BIO lies between these two cases forming reasonable interactions with PDK1, yet identifying it at a significantly poorer rank (#77) than 6BIO (#22).

To validate the prediction that PDK1 is a target for 6BIO, inhibition of PDK1 was tested in vitro: 5BIO and 7BIO cause inhibition of PDK1 only at high concentrations (IC_{50} > 100 μM) (Figure 1F). IO also showed only low potency in this regard (IC_{50} > 100 μM) (Figure 1F). In a previous publication, a certain inhibition of PDK1 by IO has already been described [6]. However, in direct comparison with IO in our experimental setting, 6BIO showed a much higher potency and classical kinetics of inhibition with an IC_{50} of about 1.5 μM (Figure 1F). Thus, in vitro testing supports our hypothesis that PDK1 is a target for 6BIO.

Biological activity of the compounds in cellular systems was assessed by examining their influence on proliferation of two different cell lines. In MCF-7 cells, 6BIO completely blocked proliferation at 10 μM (Figure 2B), while the other compounds afforded only 50% inhibition at this concentration (Figures 2A and 2C). For human endothelial cells (HMEC-1), IC_{50} values were at about 10 μM with 5BIO (Figure 2D), 3 μM with 7BIO (Figure 2F), and less than 1 μM with 6BIO (Figure 2E).

The effects of the compounds on cell proliferation could also be due to inhibition of other kinases. Therefore, we investigated endothelial cell migration as an additional functional cell-based assay, as this phenomenon has recently been shown to largely depend on PDK1 activity [24]. After defined wounding of an endothelial monolayer, migration caused complete closure of the scratch in the presence of 10% fetal calf serum within 16 hr (data not shown). In the absence of serum, the wound stayed completely open (Figures 3A and 3E). 5BIO and 7BIO caused only marginal reduction of serum-induced migration at 10 μM (Figures 3B, 3D, and 3E), while 6BIO inhibited migration by about 75% at this concentration (Figures 3C and 3E).

As a final test of in vivo activity, we determined phosphorylation of two specific downstream targets of PDK: Akt at the threonine T308 site [26] and p70S6 kinase at the threonine T229 residue [27]. Phosphorylation was determined in the absence and presence of 10 or 30 μM 5BIO,

(B) Indirubin 3′-oxime (thick, atom colored sticks) docked into a CDK2 structure. This complex has rank 1 among the kinases and rank 5 in the complete set. The model is in perfect agreement with the typical interaction motif of two or three hydrogen bonds (shown as dashed blue lines) to the protein backbone (shown in the background of this picture). The ligand originally contained in the X-ray structure is shown as thin cyan sticks for comparison.
(C) 6-bromo inidirubin 3′-oxime model into PDK1 with bound inhibitor staurosporine. The figure shows the good agreement with the backbone hydrogen bonding motif.
(D) The solvent accessible surface of the binding pocket of PDPK1 together with the VDW-Sphere depiction of 6-bromo inidirubin 3′-oxime indicate that the binding pocket can easily accommodate the halogen.
(E) 7-bromo inidirubin 3′-oxime docked into PDK1 with bound inhibitor LY333531. The binding motif is in principle present; however, the geometry of the hydrogen bonds to the backbone is not optimal.
(F) Dose-response relationships for the three compounds in the in vitro kinase assay for PDK1. 5BIO and 7BIO show inhibition only at the highest concentration tested (100 μM), whereas 6BIO shows a classical sigmoidal curve with an IC_{50} of 1.5 μM.
(G) 2D structures of the indirubin derivatives.

Table 1. The Top 25 Kinase Structures Targeted by Indirubin Derivatives According to Ligand Docking

5 BIO				6 BIO				7 BIO				IO			
PDB ID	Kinase	Score	Rank	PDB ID	Kinase	Score	Rank	PDB ID	Kinase	Score	Rank	PDB ID	Kinase	Score	Rank
1pxo_CK7	**CDK2**	−8.88	10	1q41_IXM	**GSK3B**	−8.73	4	1nb9_RBF	RIFK	−8.05	8	1pxp_CK8	**CDK2**	−9.13	5
1v0o_INR	CDC2H	−8.68	19	2bhe_BRY	**CDK2**	−8.62	5	1daw_ANP	CSK2A	−7.98	12	1pxo_CK7	**CDK2**	−8.94	6
1jvp_LIG	**CDK2**	−8.47	24	1jvp_LIG	**CDK2**	−8.50	9	1lp4_ANP	CSK2A	−7.87	13	1p2a_5BN	**CDK2**	−8.92	7
1w0x_OLO	**CDK2**	−8.46	25	1unh_IXM	**CDK5**	−8.44	10	1jvp_LIG	CDK2	−7.76	17	1p72_THM	KITH	−8.85	9
1n06_ADP	RIFK	−8.42	26	1x8b_824	WEE1	−8.34	11	1x8b_824	WEE1	−7.72	20	2bhe_BRY	**CDK2**	−8.60	14
1e9h_INR	**CDK2**	−8.39	29	1pye_PM1	**CDK2**	−8.26	12	1p72_THM	KITH	−7.60	32	1q41_IXM	**GSK3B**	−8.60	15
1pkd_UCN	**CDK2**	−8.35	31	1lp4_ANP	CSK2A	−8.24	13	1q41_IXM	GSK3B	−7.53	36	1v0o_INR	CDC2H	−8.36	28
1q41_IXM	**GSK3B**	−8.32	32	1r78_FMD	**CDK2**	−8.10	17	1w0x_OLO	CDK2	−7.51	38	1p6x_THM	KITH	−8.25	35
1lp4_ANP	CSK2A	−8.24	35	1v0o_INR	CDC2H	−8.04	18	1r0p_KSA	MET	−7.48	40	1unh_IXM	**CDK5**	−8.22	36
1fin_ATP	**CDK2**	−8.22	36	1e9h_INR	**CDK2**	−7.98	19	1pjk_ANP	CSK21	−7.47	41	1w0x_OLO	**CDK2**	−8.20	37
1x8b_824	WEE1	−8.16	41	1oky_STU	***PDK1***	−7.98	22	1day_GNP	CSK2A	−7.34	56	1pye_PM1	**CDK2**	−8.19	38
1pxp_CK8	**CDK2**	−8.11	44	1fin_ATP	**CDK2**	−7.97	23	1csn_ATP	CKI1	−7.33	58	1e9h_INR	**CDK2**	−8.15	41
1pye_PM1	**CDK2**	−8.08	50	1nb9_RBF	RIFK	−7.90	26	1om1_IQA	CSK2A	−7.33	59	1pkd_UCN	**CDK2**	−8.11	46
1vyw_292	**CDK2**	−8.05	54	1aq1_STU	**CDK2**	−7.88	27	1z57_DBQ	CLK1	−7.32	63	1x8b_824	WEE1	−8.00	51
1xbc_STU	KSYK	−8.00	60	1xbc_STU	KSYK	−7.87	29	1p2a_5BN	CDK2	−7.26	73	1n06_ADP	RIFK	−7.94	57
1nb9_RBF	RIFK	−7.92	65	1daw_ANP	CSK2A	−7.79	36	1p6x_THM	KITH	−7.16	90	1fgi_SU1	FGFR1	−7.91	59
1sm2_STU	ITK	−7.84	68	1y6a_AAZ	VGFR2	−7.77	40	1pye_PM1	CDK2	−7.14	94	1unl_RRC	**CDK5**	−7.89	61
1aq1_STU	**CDK2**	−7.74	74	1oiq_HDU	**CDK2**	−7.73	43	1pxp_CK8	CDK2	−7.13	99	1nb9_RBF	RIFK	−7.88	62
1oky_STU	***PDK1***	−7.73	77	1di8_DTQ	**CDK2**	−7.72	46	1di8_DTQ	CDK2	−7.12	100	1fin_ATP	**CDK2**	−7.87	65
1u59_STU	ZAP70	−7.72	78	1o6y_ACP	PKNB	−7.71	47	1e8z_STU	PK3CG	−6.97	134	1daw_ANP	CSK2A	−7.85	69
1oit_HDT	**CDK2**	−7.67	83	1urw_I1P	**CDK2**	−7.71	48	1oiq_HDU	CDK2	−6.95	140	1lp4_ANP	CSK2A	−7.79	79
1pjk_ANP	CSK21	−7.67	84	1uu7_BI2	***PDK1***	−7.70	50	2bhe_BRY	CDK2	−6.95	141	1pxn_CK6	**CDK2**	−7.79	80
1daw_ANP	CSK2A	−7.64	86	1p72_THM	KITH	−7.68	52	1o6y_ACP	PKNB	−6.92	150	1vyw_292	**CDK2**	−7.77	84
1h1s_4SP	**CDK2**	−7.62	90	2biy_ATP	***PDK1***	−7.61	63	1q8t_Y27	KAPCA	−6.92	151	1jvp_LIG	**CDK2**	−7.73	93
1y6a_AAZ	VGFR2	−7.60	92	1day_GNP	CSK2A	−7.59	66	2src_ANP	SRC	−6.89	162	1oky_STU	***PDK1***	−7.69	95

The respective ligands were docked to the structures from the Protein Data Base (sc-PDB). The most frequently used abbreviations in the PDB ID columns of the table are: STU (staurosporine), IXM (indirubin-3′monoxime), and ANP (phoshoaminophosphonic acid-adenylateester). When several structures were available, all were tested. The 25 kinase structures with the most favorable docking scores are listed in descending order. Known targets of each compound are shown in bold, structures of PDK1 are in bold and italics. "Rank" relates to the ranking in the complete screening from Table S1.

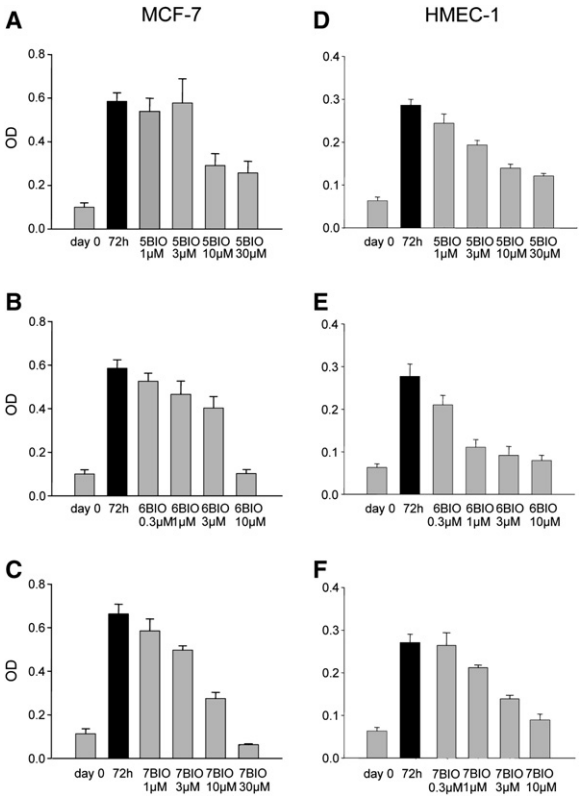

Figure 2. Effects of Indirubin Derivatives on Proliferation

MCF-7 cells (A–C) and HMEC-1 cells (D–F) were observed after 72 hr growth in the absence or presence of the indicated compounds. Proliferation was measured colorimetrically (OD) by using the crystal violet assay. Error bars denote standard error of the mean taken from three measurements with three replicas each.

6BIO, and 7BIO, respectively, in MCF-7 cells. Since phosphorylation of both substrates is significantly inhibited by 6BIO, but not by 5BIO or 7BIO in both cell types (Figure 3G), we can conclude that 6BIO, in contrast to 5BIO and 7BIO, indeed inhibits PDK1 in vivo at micromolar concentrations.

We have shown that inverse virtual screening is able to specifically identify cellular targets for small molecules. Furthermore, in this case, the approach correctly identified 6BIO as the compound interacting best with PDK1, thus having qualitatively predicted differences between very similar compounds. The combined approach described here may serve to accelerate and simplify the drug discovery and development process, and to study the biological activity profiles of already known and established kinase inhibitors. This is still an important issue, as has recently been shown for LY294002, a well established PI3 kinase inhibitor: by a work-intensive proteomics approach, this compound was found to interact with a vast number of off-target kinases [28].

Compared to purely experimental approaches for finding targets, inverse screening has the advantage of applicability across protein families and functional relevance. Chemical proteomics approaches [28] have the disadvantage that they only test for binding, not for functionally relevant interactions. Large scale binding affinity assays require family specific reference ligands for the competition assay. Inverse screening is less resource intensive; however, it has the main drawback of the prediction error, thus requiring experimental validation of predictions, e.g., in the type of vertical approach demonstrated in this work. As such, it is a valuable complementary approach to current experimental techniques for identifying new targets and can be useful in understanding potential drug side effects, identifying new applications for existing compounds [29], and interpreting phenotypes induced by a compound in chemical biology experiments [30].

SIGNIFICANCE

Typical in vitro screening assays for small molecules only allow testing against one defined target protein. Thus, potential side effects (or other more important targets) may be overlooked. In inverse virtual screening, a high number of protein structures from a protein data base are virtually tested for inhibitor binding. As far as we know, we have for the first time applied this approach to kinases, which comprise a class of proteins that are most attractive drug targets. This process has led to the identification of the kinase PDK1 as an as-yet-unknown target of the indirubin derivative 6BIO. In addition, we were able to validate our in vitro prognosis in cellular systems. We conclude that this approach of inverse in vitro screening could be a valuable tool for facilitating and accelerating the drug discovery process.

EXPERIMENTAL PROCEDURES

Virtual Inverse Screening

For the structure based virtual screening, the scPDB database of binding sites was used. Our version contains 5,834 protein structures, representing 1,435 unique proteins, when the source organism is neglected. Kinase structures were identified by extracting from the protein structure database scPDB [31] all complexes annotated with an EC number beginning with 2.7.1.*. The resulting set of kinase structures contained 327 complexes, representing 84 unique proteins, when the source organism is neglected. All three compounds used in this study were docked into each protein structure with the docking tool GlamDock [32]. The active site for each docking was defined as a sphere of radius 9A centered on the bound ligand as contained in the scPDB. Docking was performed under the assumption of a rigid binding site; however, structural variation in kinase structure is partially accommodated for by the presence of multiple X-ray structures for several kinases in complex with different ligands.

The ligands were docked with the standard ChillScore function used for docking in GlamDock [32]. GlamDock is a Monte Carlo with Minimization [33]-based docking algorithm, which combines a number of previously suggested methods to obtain high accuracy and high efficiency predictions. The Monte Carlo search uses a probe based approach for defining the ligand orientation and an internal coordinate (torsions) description of ligand conformation. At each step, both orientation and conformation are changed by a small perturbation, and the ligand is placed into the binding site according to the new coordinates. A subsequent torsion space minimization with the full energy function is performed for 15 steps, to relax the conformation in the field of the protein. The ensuing conformation is retained or discarded according to the Metropolis criterion.

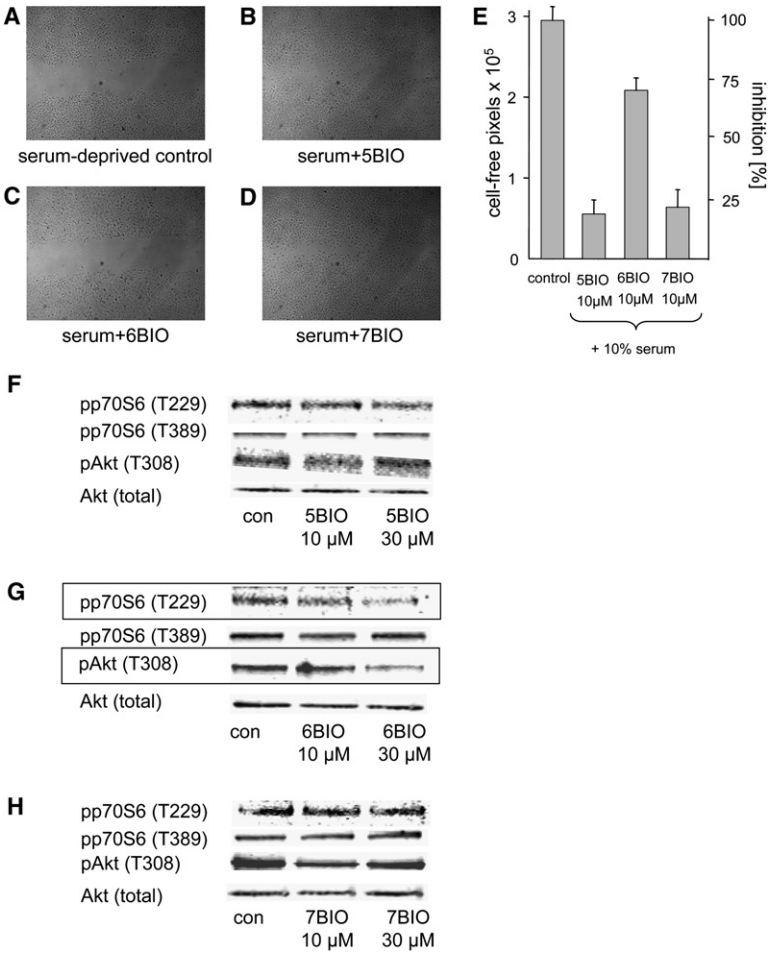

Figure 3. Endothelial Cell Migration Is Most Potently Inhibited by 6BIO

In the scratch wound, migration assay with endothelial cells complete wound closure is observed in the presence of 10% serum (data not shown). In the absence of serum, the gap remains open (A). 5BIO and 7BIO did only moderately influence migration (B and D), while 6BIO elicited 75% inhibition (C). (E) Quantitative evaluation. Error bars denote standard error of the mean taken from three measurements with three replicas each. (F–H) 6BIO inhibits phosphorylation of PDK1-specific sites in p70S6 kinase (T229) and Akt (T308) in MCF-7 cells. In contrast to 5BIO (F) and 7BIO (H), 6BIO (G) inhibits phosphorylation of PDK1-specific targets (indicated by boxes). An irrelevant phosphorylation site at T389 in p70S6 and overall content of Akt remain unchanged (F–H).

A docking simulation consists of five simulated annealing runs of 300 Monte Carlo steps each, where local minima are kept during all simulations, pose clustered and postminimized with 80 steps of torsion space minimization. A docking simulation takes approximately 1 min on a standard PC CPU. The best ranking conformation is predicted as the structure of the complex. The energy function used for the minimization and for ranking the conformations is ChillScore, which is a continuous, differentiable empirical potential derived by fitting interaction energies to binding affinities of known complexes. More details on the algorithm, the energy function, and a wide ranging validation are given elsewhere [32]. For the ranking of the different putative complexes a second variant of the scoring function was used, which neglects interactions with metal ions present in the kinase active site.

As indirubin-3′-oxime is not known to interact with metal ions, we assumed that such interactions would also not occur in the binding modes of the halogenated derivatives. Interactions with metal ions are, however, strongly favored by standard empirical scoring functions, and ChillScore is no exception to this rule. The reason for this preference is that empirical scoring functions do not punish metal ligand interactions of poor geometry and do not take competition with water for metal ligand sites correctly into account. The bias toward formation of ligand-metal interactions leads to false hits in the inverse screening since structures showing such interactions tend to rank well. To remove this bias from the ranking, the structural models resulting from the docking procedure were reranked by a specialized energy function that ignores ligand-metal ion interactions. This energy function, a variant of the empirical ChillScore energy function used for docking [32], was derived by performing a two-step least-squares fit on the complexes and binding affinities reported in the PDBBind database without using the metal-acceptor interaction term. For each inhibitor, the kinase structures were then sorted in order of increasing predicted binding free energy (decreasing affinity) for each complex (Table 1).

In Vitro Kinase Assay

PDK1 protein kinase was expressed in Sf9 insect cells as human recombinant GST-fusion protein by means of the baculovirus expression system. The kinase was purified by affinity chromatography with GSH-agarose. The purity of the kinase was checked by SDS-PAGE/silver staining, and the identity was verified by mass spectroscopy. A proprietary protein kinase assay (^{33}PanQinase assay) was used for measuring the kinase activity of PDK1. All kinase assays were performed in 96-well FlashPlates from Perkin Elmer/NEN (Boston, MA, USA) in a 50 μl reaction volume. The assay for PDK1 contained 60 mM HEPES-NaOH (pH 7.5), 3 mM $MgCl_2$, 3 mM $MnCl_2$, 3 μM Na-orthovanadate, 1.2 mM DTT, 50 μg/ml PEG_{20000}, 1 μM [γ-^{33}P]-ATP (approx. 5 × 10^5 cpm per well). The reaction cocktails were incubated at 30°C for 80 min. The reaction was stopped with 50 μl of 2% (v/v) H_3PO_4, and plates were aspirated and washed two times with 200 μl 0.9% (w/v) NaCl. Incorporation of $^{33}P_i$ was determined with a microplate scintillation counter (Microbeta, Wallac). The residual activities for each concentration and the compound IC_{50} values were calculated with Quattro Workflow V2.0.2.2 (Quattro Research GmbH, Munich, Germany). The model used was "Sigmoidal response (variable slope)" with parameters "top" fixed at 100% and "bottom" at 0%.

Cell Culture

The breast cancer cell line MCF-7 was routinely cultured in RPMI medium supplemented with 10% FCS. Human microvascular endothelial cells (HMEC-1) were a kind gift by Dr. F.J. Candal from the CDC, Atlanta, GA, USA. Theses cells were cultured in endothelial growth medium (Provitro, Berlin, FRG) supplemented with 10% serum. Primary endothelial cells (HUVECs) were isolated from umbilical veins by collagenase digestion. Cells were used at passage two or three.

Proliferation Assay

Proliferation of MCF-7 cells or HMEC-1 was examined by using crystal violet as described in the NCI protocols. Briefly, cells are detached by trypsinization and seeded at a density of 1,500 per well in 96-well dishes. After 24 hr, one plate is stained with crystal violet, washed, and air dried (day 0), the other plates are incubated with the respective compounds for 72 hr. After this time, the plates are also stained and dried, the stain is eluted with ethanol and citrate, and absorbance is measured at 540 nm. Absorption linearly correlates with cell number.

Migration Assay

Confluent HUVEC monolayers were wounded by scratching with a 100 μl pipette tip. Cells were treated with the respective compound or solvent for 16 hr. The degree of wound closure after this time was examined microscopically and quantified by using a specially developed software (S.CO LifeScience, Garching, FRG).

Western Blot Analysis

Lysis of MCF-7 or HMEC-1 cells and gel electrophoresis was performed by standard procedures. The following primary antibodies were used: rabbit anti-phospho-p70S6 kinase (T229) from R&D systems, rabbit anti-phospho-p70S6 kinase (T389) from Cell Signaling, rabbit anti-phospho-Akt (T308) from Cell Signaling, and rabbit anti-Akt from Cell Signaling. The respective protein was detected by using fluorescent-labeled secondary antibodies and analysis in an infrared scanner (Odyssey, LI-COR Biosciences, Bad Homburg, Germany).

Statistical Analysis

All experiments were performed in triplicates at least in three independent sets of experiments. For western blots, one representative blot is shown. All quantitative data are presented as mean ± standard error of the mean (SEM). For comparisons with control, one way ANOVA was used. As a post-hoc test, we used the Student-Newman-Keuls procedure.

Supplemental Data

Supplemental Data include a table of the screening results over the complete protein database for the four compounds (5BIO, 6BIO, 7BIO, and IOX) and are available at http://www.chembiol.com/cgi/content/full/14/11/1207/DC1/.

ACKNOWLEDGMENTS

This work was in part supported by a grant of the European Community (FP6-2002-Life Sciences & Health, PRO-KINASE Research Project, project number LSHB-CT-2004-503467) and German Research Council (Deutsche Forschungsgemeinschaft) project AP101/1.

Received: August 9, 2007
Revised: September 17, 2007
Accepted: October 10, 2007
Published: November 26, 2007

REFERENCES

1. Dancey, J., and Sausville, E.A. (2003). Issues and progress with protein kinase inhibitors for cancer treatment. Nat. Rev. Drug Discov. *2*, 296–313.
2. Sebolt-Leopold, J.S., and Herrera, R. (2004). Targeting the mitogen-activated protein kinase cascade to treat cancer. Nat. Rev. Cancer *4*, 937–947.
3. Hynes, N.E., and Lane, H.A. (2005). ERBB receptors and cancer: the complexity of targeted inhibitors. Nat. Rev. Cancer *5*, 341–354.
4. Faivre, S., Kroemer, G., and Raymond, E. (2006). Current development of mTOR inhibitors as anticancer agents. Nat. Rev. Drug Discov. *5*, 671–688.
5. Granville, C.A., Memmott, R.M., Gills, J.J., and Dennis, P.A. (2006). Handicapping the race to develop inhibitors of the phosphoinositide 3-kinase/Akt/mammalian target of rapamycin pathway. Clin. Cancer Res. *12*, 679–689.
6. Bain, J., McLauchlan, H., Elliott, M., and Cohen, P. (2003). The specificities of protein kinase inhibitors: an update. Biochem. J. *371*, 199–204.
7. Knight, Z.A., and Shokat, K.M. (2005). Features of selective kinase inhibitors. Chem. Biol. *12*, 621–637.
8. Fabian, M.A., Biggs, W.H., III, Treiber, D.K., Atteridge, C.E., Azimioara, M.D., Benedetti, M.G., Carter, T.A., Ciceri, P., Edeen, P.T., Floyd, M., et al. (2005). A small molecule-kinase interaction map for clinical kinase inhibitors. Nat. Biotechnol. *23*, 329–336.
9. Chen, Y.Z., and Zhi, D.G. (2001). Ligand-protein inverse docking and its potential use in the computer search of protein targets of a small molecule. Proteins *43*, 217–226.
10. Paul, N., Kellenberger, E., Bret, G., Muller, P., and Rognan, D. (2004). Recovering the true targets of specific ligands by virtual screening of the protein data bank. Proteins *54*, 671–680.
11. Steffen, A., Thiele, C., Tietze, S., Strassnig, C., Kamper, A., Lengauer, T., Wenz, G., and Apostolakis, J. (2007). Improved cyclodextrin-based receptors for camptothecin by inverse virtual screening. Chemistry *13*, 6801–6809.
12. MacDonald, M.L., Lamerdin, J., Owens, S., Keon, B.H., Bilter, G.K., Shang, Z., Huang, Z., Yu, H., Dias, J., Minami, T., et al. (2006). Identifying off-target effects and hidden phenotypes of drugs in human cells. Nat. Chem. Biol. *2*, 329–337.
13. Bradbury, J. (2005). From Chinese medicine to anticancer drugs. Drug Discov. Today *10*, 1131–1132.
14. Meijer, L., Skaltsounis, A.L., Magiatis, P., Polychronopoulos, P., Knockaert, M., Leost, M., Ryan, X.P., Vonica, C.A., Brivanlou, A., Dajani, R., et al. (2003). GSK-3-selective inhibitors derived from Tyrian purple indirubins. Chem. Biol. *10*, 1255–1266.
15. Eisenbrand, G., Hippe, F., Jakobs, S., and Muehlbeyer, S. (2004). Molecular mechanisms of indirubin and its derivatives: novel anticancer molecules with their origin in traditional Chinese phytomedicine. J. Cancer Res. Clin. Oncol. *130*, 627–635.
16. Ribas, J., Bettayeb, K., Ferandin, Y., Knockaert, M., Garrofe-Ochoa, X., Totzke, F., Schachtele, C., Mester, J., Polychronopoulos, P., Magiatis, P., et al. (2006). 7-Bromoindirubin-3′-oxime induces caspase-independent cell death. Oncogene *25*, 6304–6318.
17. Okamoto, K., and Sagata, N. (2007). Mechanism for inactivation of the mitotic inhibitory kinase Wee1 at M phase. Proc. Natl. Acad. Sci. USA *104*, 3753–3758.
18. Xie, Z., Yuan, H., Yin, Y., Zeng, X., Bai, R., and Glazer, R.I. (2006). 3-phosphoinositide-dependent protein kinase-1 (PDK1) promotes invasion and activation of matrix metalloproteinases. BMC Cancer *6*, 77.
19. Lin, H.J., Hsieh, F.C., Song, H., and Lin, J. (2005). Elevated phosphorylation and activation of PDK-1/AKT pathway in human breast cancer. Br. J. Cancer *93*, 1372–1381.
20. Mora, A., Komander, D., van Aalten, D.M., and Alessi, D.R. (2004). PDK1, the master regulator of AGC kinase signal transduction. Semin. Cell Dev. Biol. *15*, 161–170.

21. Berven, L.A., Willard, F.S., and Crouch, M.F. (2004). Role of the p70(S6K) pathway in regulating the actin cytoskeleton and cell migration. Exp. Cell Res. *296*, 183–195.

22. Chen, J., Somanath, P.R., Razorenova, O., Chen, W.S., Hay, N., Bornstein, P., and Byzova, T.V. (2005). Akt1 regulates pathological angiogenesis, vascular maturation and permeability in vivo. Nat. Med. *11*, 1188–1196.

23. Phung, T.L., Ziv, K., Dabydeen, D., Eyiah-Mensah, G., Riveros, M., Perruzzi, C., Sun, J., Monahan-Earley, R.A., Shiojima, I., Nagy, J.A., et al. (2006). Pathological angiogenesis is induced by sustained Akt signaling and inhibited by rapamycin. Cancer Cell *10*, 159–170.

24. Primo, L., di Blasio, L., Roca, C., Droetto, S., Piva, R., Schaffhausen, B., and Bussolino, F. (2007). Essential role of PDK1 in regulating endothelial cell migration. J. Cell Biol. *176*, 1035–1047.

25. Hinton, H.J., Alessi, D.R., and Cantrell, D.A. (2004). The serine kinase phosphoinositide-dependent kinase 1 (PDK1) regulates T cell development. Nat. Immunol. *5*, 539–545.

26. Alessi, D.R., James, S.R., Downes, C.P., Holmes, A.B., Gaffney, P.R., Reese, C.B., and Cohen, P. (1997). Characterization of a 3-phosphoinositide-dependent protein kinase which phosphorylates and activates protein kinase Balpha. Curr. Biol. *7*, 261–269.

27. Pullen, N., Dennis, P.B., Andjelkovic, M., Dufner, A., Kozma, S.C., Hemmings, B.A., and Thomas, G. (1998). Phosphorylation and activation of p70s6k by PDK1. Science *279*, 707–710.

28. Gharbi, S.I., Zvelebil, M.J., Shuttleworth, S.J., Hancox, T., Saghir, N., Timms, J.F., and Waterfield, M.D. (2007). Exploring the specificity of the PI3K family inhibitor LY294002. Biochem. J. *404*, 15–21.

29. Ashburn, T.T., and Thor, K.B. (2004). Drug repositioning: identifying and developing new uses for existing drugs. Nat. Rev. Drug Discov. *3*, 673–683.

30. Peters, U., Cherian, J., Kim, J.H., Kwok, B.H., and Kapoor, T.M. (2006). Probing cell-division phenotype space and Polo-like kinase function using small molecules. Nat. Chem. Biol. *2*, 618–626.

31. Kellenberger, E., Muller, P., Schalon, C., Bret, G., Foata, N., and Rognan, D. (2006). sc-PDB: an annotated database of druggable binding sites from the Protein Data Bank. J. Chem. Inf. Model. *46*, 717–727.

32. Tietze, S., and Apostolakis, J. (2007). Glamdock: development and validation of a new docking tool on several thousand protein-ligand complexes. J. Chem. Inf. Model. *47*, 1657–1672.

33. Apostolakis, J., Plückthun, A., and Caflisch, A. (1998). Docking small ligands in flexible binding sites. J. Comput. Chem. *19*, 21–37.

